Clim. Past Discuss., 9, 1–41, 2013
www.clim-past-discuss.net/9/1/2013/
doi:10.5194/cpd-9-1-2013
© Author(s) 2013. CC Attribution 3.0 License.

Climate of the Past Discussions

This discussion paper is/has been under review for the journal Climate of the Past (CP).
Please refer to the corresponding final paper in CP if available.

Holocene climate variations in the western Antarctic Peninsula: evidence for sea ice extent predominantly controlled by insolation and ENSO variability changes

J. Etourneau[1,*], L. G. Collins[1], V. Willmott[2], J. H. Kim[2], L. Barbara[3], A. Leventer[4], S. Schouten[2], J. S. Sinninghe Damsté[2], A. Bianchini[4], V. Klein[1], X. Crosta[3], and G. Massé[1]

[1]Laboratoire d'Océanographie et du Climat: Expérimentations et Approches Numériques, UMR7159, CNRS/UPMC/IRD/MNHN, 4 Place Jussieu, 75252 Paris, France
[2]Royal Netherlands Institute for Sea Research, Department of marine Biogeochemistry and toxicology, 1790 Den Burg, Texel, The Netherlands
[3]EPOC, UMR5805, CNRS, Université Bordeaux 1, Avenue des Facultés, 33405 Talence, France
[4]Colgate University, Department of Geology, 13 Oak Drive, 13346 Hamilton, USA
[*]current address: Institute of Biogeosciences, Japan Agency for Marine-Earth Science and Technology, 2-15 Natsushima-cho, Yokosuka, 237-0061, Japan

Received: 6 December 2012 – Accepted: 18 December 2012 – Published: 2 January 2013

Correspondence to: J. Etourneau (johan.etourneau@locean-ipsl.upmc.fr)

Published by Copernicus Publications on behalf of the European Geosciences Union.

Abstract

The West Antarctic ice sheet is particularly sensitive to global warming and its evolution and impact on global climate over the next few decades remains difficult to predict. In this context, investigating past sea ice conditions around Antarctica is of primary importance. Here, we document changes in sea ice presence, upper water column temperatures (0–200 m) and primary productivity over the last 9000 yr BP (before present) in the western Antarctic Peninsula (WAP) margin from a sedimentary core collected in the Palmer Deep basin. Employing a multi-proxy approach, we derived new Holocene records of sea ice conditions and upper water column temperatures, based on the combination of two biomarkers proxies (highly branched isoprenoid (HBI) alkenes for sea ice and TEX_{86}^{L} for temperature) and micropaleontological data (diatom assemblages). The early Holocene (9000–7000 yr BP) was characterized by a cooling phase with a short sea ice season. During the mid-Holocene (~ 7000–3000 yr BP), local climate evolved towards slightly colder conditions and a prominent extension of the sea ice season occurred, promoting a favorable environment for intensive diatom growth. The late Holocene (the last ~ 3000 yr) was characterized by more variable temperatures and increased sea ice presence, accompanied by reduced local primary productivity likely in response to a shorter growing season compared to the early or mid-Holocene. The stepwise increase in annual sea ice duration over the last 7000 yr might have been influenced by decreasing mean annual and spring insolation despite an increasing summer insolation. We postulate that in addition to precessional changes in insolation, seasonal variability, via changes in the strength of the circumpolar Westerlies and upwelling activity, was further amplified by the increasing frequency/amplitude of El Niño-Southern Oscillation (ENSO). However, between 4000 and 2100 yr BP, the lack of correlation between ENSO and climate variability in the WAP suggests that other climatic factors might have been more important in controlling WAP climate at this time.

CPD
9, 1–41, 2013

1 Introduction

The Antarctic seasonal sea ice cycle impacts ocean-atmosphere heat and gas fluxes (Anderson et al., 2009), the formation of deep and intermediate waters that participate in driving the thermohaline circulation (e.g. Orsi et al., 2002), biogeochemical cycles and local biological production (Marinov et al., 2006; Sarmiento et al., 2004; Toggweiler et al., 2006). The Antarctic seasonal sea ice cycle is strongly affected by recent warming, especially in the western Antarctic sector where the seasonal duration of sea ice has decreased by over 85 ± 20 days between 1979 and 2004 (Stammerjohn et al., 2008). In the WAP, global warming has had a stronger and faster effect than in any other region of Antarctica (Vaughan et al., 2003; Steig et al., 2009). For instance, the WAP has experienced a winter air warming trend of almost 6 °C since the 1950's (King et al., 1994), which have been associated with increasingly reduced duration of winter sea ice cover (Stammerjohn et al., 2008), and the widespread retreat of WAP ice shelves (Doake and Vaughan, 1991; Rott et al., 1996; Vaughan and Doake, 1996). Subsurface ocean warming of +0.3 °C (the 0–300 m upper layer) over the last century (Levitus et al., 2000) strongly affects ice shelf stability in some sectors of West Antarctica and has the potential to significantly increase global sea-level (King, 1994; Joughin and Alley, 2011; Rignot, 2006).

Bentley et al. (2009) provide a comprehensive review of Holocene paleoclimate records from the Antarctic Peninsula, including data from ice cores, and lacustrine and marine sediment cores. Similarly, Taylor and Sjunneskog (2002) and Allen et al. (2010) summarized existing proxy data sets. These records, which show some regional variability in the timing and expression of the climate signal, document two warm periods, the first during the early Holocene and the second, during the "MidHolocene Hypsithermal" (Bentley et al., 2009). Recent marine geochemical data from the Palmer Deep (WAP) based on the TEX_{86} proxy, similarly document a relatively warm early Holocene (Shevenell et al., 2011), with average sea surface temperature (SST) of 3.7 ± 2.2 °C between 11 800 and 9000 yr BP and some peaks reaching +10 °C, followed

CPD
9, 1–41, 2013

by millennial-scale variability of SST superimposed on an overall cooling of 3–4 °C throughout the Holocene. More recently, a newly published ice core record from James Ross Island, Eastern Antarctic Peninsula (Mulvaney et al., 2012) also documents a warm early Holocene, with atmospheric temperatures approximately $+1.3 \pm 0.3$ °C warmer than today. The ice core record revealed relatively cooling temperatures of ~1 °C from ~9200 to 5000 yr BP, with a slowdown or slightly warmer temperatures from ~5000 to 3000 yr BP corresponding to the "MidHolocene Hypsithermal", before a second cooling step of ~1 °C over the late Holocene.

Here, we provide a new multi-proxy record from a core located in the Palmer Deep Basin (WAP) on the continental open shelf, south of Anvers Island. We combine more traditional diatom assemblage data with more recent developments in multi-proxy analytical work, including a temperature record based on the well-calibrated TEX_{86}^{L} paleothermometer, and a high-resolution record of specific diatom biomarker lipids, the highly branched isoprenoid (HBI) alkenes, which are directly related to sea ice variability. Combining these records has enabled us to assess Holocene climatic changes in the central part of the WAP, to compare our new data with other records from the region, including those from the nearby ODP Site 1098, also in the Palmer Deep (Domack et al., 2001; Leventer et al., 1996, 2002; Shevenell and Kennett, 2002; Sjunneskog and Taylor, 2002; Taylor and Sjunneskog, 2002; Ishman and Sperling, 2002; Shevenell et al., 2001), and to test hypotheses presented previously to explain WAP climate fluctuations over the last 9000 yr BP (insolation and ENSO) (e.g. Shevenell et al., 2011).

2 Oceanographic setting

The northern WAP is influenced by the Southern Ocean Westerlies and the Antarctic Circumpolar Current (ACC) (Fig. 1). The ACC mainly transports Circumpolar Deep Water (CDW) (Sievers and Nowlin, 1984), which is a relatively warm water mass and comprises an upper branch, the Upper Circumpolar Deep Water (UCDW), an oxygen minimum and high nutrient concentration layer, and a lower branch, the Lower Circumpolar

CPD
9, 1–41, 2013

Deep Water with a salinity maximum (Rintoul et al., 2001). CDW is derived from a mixture of deep waters arising from the North Atlantic, Pacific and Indian Oceans as well as waters formed in the Antarctic region. Due to Ekman pumping, CDW upwells onto the shelf when strong Westerlies are displaced south and penetrates the WAP shelf via deep glacial troughs (Klinck et al., 2004). In addition, strong offshore winds during the sea ice retreat season cause the relatively warm and salty UCDW (1.5 °C, 34.6–34.73 psu (Moffat et al., 2008)) to mix with Antarctic Surface Water (AASW). AASW forms in the upper 100–150 m of the water column and is mostly controlled by ice formation and melting, as well as wind forcing (Dierssen et al., 2002). AASW differs from UCDW by its cold temperatures and relatively low salinity (between −1.8 and 1 °C, 33.0–33.7 psu) (Smith et al., 1999). During the ice-free season, the modified UCDW upwells heat and nutrients, which are important for biological productivity (e.g. Moffat et al., 2008). The vertical transport of relatively warm UCDW is believed to prevent high rates of sea ice production along the WAP shelf (Martinson et al., 2008).

Satellite monitoring demonstrates large spatial and temporal variability of sea ice along the WAP (Stammerjohn and Smith, 1996) and significant changes in sea ice duration over the past several decades (Stammerjohn et al., 2008a; 2008b). While mean winter sea ice limits are located between 60–63° S, the average summer sea ice boundary lies between 67–69° S, 3–4° south of Anvers Island (Fig. 1). There is little ice coverage during the austral summer, between January and April, with a minimum in March (Stammerjohn and Smith, 1996). Sea ice grows during the austral autumn and reaches its maximum cover in August (Stammerjohn and Smith, 1996), before melting between September and November. During the spring sea ice melt season, when temperatures warm, injections of fresh water, from the melting sea ice, stratify the water column, trap nutrients and phytoplankton in the light-rich photic zone and promote widespread primary production dominated by spring bloom diatom assemblages (Annett et al., 2010). Later in the summer season, brine-rich waters are mixed, by the Westerlies and associated extratropical cyclonic flow, with deeper and warmer upwelled waters, which renew the nutrient pool and promote a second phytoplankton bloom (Moffat et al., 2008).

CPD
9, 1–41, 2013

3 Materials and methods

We generated Holocene records by analyzing sediment slices of the Jumbo Piston Core 10 (JPC-10), collected during the United States Antarctic Program Cruise 03 in 1999 by the R/V *Nathaniel B. Palmer*. NBP9903 JPC-10 core, 13.33 m long and mainly composed of diatomaceous mud, was obtained from the Palmer Deep basin (64°53′ S, 64°12′ W, 905 m water depth), south of the Anvers Island, close to the ODP (Ocean Drilling Program) Site 1098 (64°51′ S, 64°12′ W, 1010 m water depth) (Fig. 1). We also analyzed 19 sediment samples of the core drilled at the latter site for comparison with the record of Shevenell et al. (2011). Sedimentary structures and physical properties of the JPC-10 core are discussed in Domack et al. (2003) where they showed that sediments are not disturbed by turbidites.

3.1 Age model

The age model for JPC-10 was primarily based on the correlation of its magnetic susceptibility (MS) with the MS recorded at ODP Site 1098, which in turn has a robust age-model derived from 54 ^{14}C dates (Domack et al., 2001). The two MS records show remarkably similar trends throughout the Holocene (Fig. 2). Correlation of the MS records of the two cores was further controlled by two carbonate-based radiocarbon dates from JPC-10. These two ^{14}C dates at 1250 cm and 1323 cm were corrected using a 1230 yr regional age reservoir (Domack et al., 2001) and calibrated using the Calib 6.1.1 radiocarbon calibration program, thus corresponding to 8404 and 9040 yr BP, respectively. The good correlation between the NBP9903 JPC-10 and ODP Site 1098 allows for the reconstruction of Holocene variability at a centennial scale. According to the stratigraphy used, the top of the JPC-10 core corresponds to ∼270 yr BP within the age model uncertainties. The sedimentation rate (SR) is 0.1–0.15 cm yr^{-1} between 9000 and 8000 yr BP and again for the last 5000 yr BP, while during the intervening period, between 8000–5000 yr BP, the SR is higher, ranging between 0.2–0.3 cm yr^{-1}.

CPD
9, 1–41, 2013

3.2 Proxies

3.2.1 Biomarkers extraction

For isoprenoid glycerol dibiphytanyl glycerol tetraethers (GDGTs) and highly branched isoprenoids (HBI) alkenes, lipids were first extracted at the Laboratoire d'Océanographie et du Climat: Experimentations et Approches Numériques (LOCEAN) using a mixture of 9 mL CH_2Cl_2/MeOH (2 : 1, v : v) to which internal standards (7 hexyl nonadecane, 9 octyl heptadecene and androstanol) were added. Several sonication and centrifugation steps were applied in order to properly extract the desired compounds. After drying with N_2 at 35 °C, the total lipid extract was fractionated over a silica column into an apolar and a polar fraction using 3 mL hexane and 6 mL CH_2Cl_2/MeOH (1 : 1, v : v), respectively.

3.2.2 TEX_{86}^{L}

The TEX_{86} (TetraEther Index of tetraethers with 86 carbon atoms) proxy is based on the relative distribution of *Thaumarchaeotal* lipids or GDGTs (Schouten et al., 2002). For temperature reconstruction, we measured TEX_{86}^{L} at a centennial scale resolution. TEX_{86}^{L} is the modified form of TEX_{86} and is recommended for application in polar oceans (Kim et al., 2010). In contrast to a previous study in the WAP (Shevenell et al., 2011) which adapted the original TEX_{86} proxy and performed a local calibration, we used TEX_{86}^{L} as a proxy for reconstructing paleotemperature at the JPC-10 core site. Correlation of the TEX_{86} index with SST < 10 °C, i.e. in the polar oceans, shows that changes in TEX_{86} are relatively minor with temperature and therefore this index is likely unsuitable for polar regions (Kim et al., 2008). Kim et al. (2010) readdressed the relationship of GDGTs with SST leading to the definition of a new GDGT index, TEX_{86}^{L}

$$TEX_{86}^{L} = \log\left(\frac{[\text{GDGT-2}]}{[\text{GDGT-1}] + [\text{GDGT-2}] + [\text{GDGT-3}]}\right) \quad (1)$$

CPD
9, 1–41, 2013

GDGT-1, GDGT-2, and GDGT-3 indicate GDGTs containing 1, 2, and 3 cyclopentane moieties, respectively.

Since *Thaumarchaeota* are in low abundance in the Antarctic summer surface water (the ∼0–45 m layer of low salinity water mass) but more abundant in winter in the ∼45–105 m depth interval of cold, salty water (i.e. the summer remnant of the previous winter, surface-mixed layer) (Kalanetra et al., 2009), we used the TEX^{L}_{86} calibration established against the integrated 0–200 m water depth temperatures (see Kim et al., 2012):

$$T = 50.8 \times TEX^{L}_{86} + 36.1 (r^2 = 0.87, n = 396, p < 0.0001, 0\text{–}200\,\text{m}) \quad (2)$$

It is also worthwhile to note that *Thaumarchaeota* are found in Antarctic sea ice (Cowie et al., 2011), albeit in low abundance and below the sea ice (Alonso-Sáez et al., 2012; Grzymski et al., 2012). This shows that their production may occur even below the freezing point of water (i.e. < 0 °C). The application of TEX^{L}_{86} on the JPC-10 core results in a 1.2 °C temperature estimate for the most recent sediment (see results), which is within the range of the present annual mean temperature between 0–200 m at this location (Martinson et al., 2008). Thus, this proxy seems to be appropriate for the reconstruction of temperature in sediment records from polar oceans with an associated residual standard error of ± 2.8 °C (Kim et al., 2012). In order to depict a regional temperature pattern in the WAP, we also analyzed 19 samples from core ODP 1098 (Hole B) for which Shevenell et al. (2011) already reported TEX_{86} temperature estimates.

Prior to analysis, the collected polar fraction, containing the GDGTs, was redissolved by sonication (5 min) in a *n*-hexane : 2-propanol (99 : 1, v : v) solvent mixture, and filtered through 0.45 µm PTFE filters at the Royal Netherlands Institute for Sea Research (NIOZ). GDGT analyses were performed using an Agilent (Palo-Alto, CA, USA) 1100 series LC-MS equipped with an auto-injector and Chemstation chromatography manager software (see Hopmans et al., 2000; Schouten et al., 2007). Separation was achieved on a Prevail Cyano column (2.1 × 150 mm, 3 m; Alltech, Deerfield, IL, 150 USA), maintained at 30 °C and an injection volume of 1 µL. GDGTs were

CPD
9, 1–41, 2013

eluted isocratically with 99 % A and 10 % B for 5 min, followed by a linear gradient to 16 % B in 45 min, where A = hexane and B = hexane/propanol (9 : 1, v : v). Flow rate was 0.2 mL min^{-1}. After each analysis the column was cleaned by back-flushing hexane/propanol (9 : 1, v : v) at 0.2 mL min^{-1} for 10 min. Detection was achieved using atmospheric pressure positive ion chemical ionization mass spectrometry (APCI-MS). Conditions for the HP 1100 APCI-MS were as follows: nebulizer pressure 60 psi, vaporizer temperature 400 °C, drying gas (N_2) flow 6 L min^{-1} and temperature 200 °C, capillary voltage −3 kV, corona 5 A (∼ 3.2 kV). GDGTs were detected by Selected Ion Monitoring (SIM) of their $[M + H]^+$ ions (dwell time = 234 ms) (Schouten et al., 2007). Fractional abundances of each isoprenoid GDGT were obtained by normalizing each peak area to the summed area of all six isoprenoid GDGTs.

3.2.3 Highly Branched Isoprenoids (HBIs)

The concentrations of di and tri-unsaturated HBI lipids (respectively, $C_{25:2}$ and $C_{25:3}$ HBI alkenes), which are diatom-specific biomarkers (Volkman et al., 1994), were determined at a decadal scale resolution, within age uncertainties, to reconstruct variations in past sea ice extent. It has been demonstrated that a di-unsaturated isomer (diene) is mainly synthesized by sea ice diatom species (Johns et al., 1999; Massé et al., 2011) whilst a tri-unsaturated HBI (triene) is produced by some open water diatom species (Belt et al., 2000; Massé et al., 2011). Recent studies have highlighted the potential for the application of HBIs as sea ice indicators in the Southern Ocean (Barbara et al., 2010; Denis et al., 2010; Massé et al., 2011). Determination of the ratio of the diene and triene (D/T) HBI alkenes, combined with diatom assemblage data, provides an indication of the relative input of sea ice algae and open water phytoplankton to the sediment. This new proxy has recently been applied to the reconstruction of Antarctic paleoenvironments and used to monitor the onset of deglaciation in Prydz Bay (Barbara et al., 2010), and the sea ice evolution through the Holocene in the Adélie Basin (Denis et al., 2010). Bacterial degradation is considered to have had minor effects given the good preservation of HBI over the last 60 000 yr (Collins et al., unpublished data)

CPD
9, 1–41, 2013

and their coherent evolution with diatom assemblages (Barbara et al., 2010; Denis et al., 2010). Furthermore, HBI structures appear to be relatively resistant to degradation (Robson and Rowland, 1988) although they might undergo rapid sulfurization under highly anoxic conditions (e.g. in the Antarctic Ellis fjord; Sinninghe Damsté et al., 2007). While some sedimentary sulfur species were identified at certain depths in JPC-10 sediments, GC-MS analyses did not identify any organic sulfur compounds with an HBI carbon skeleton. We are therefore relatively confident that degradation is minimal throughout the core.

HBIs were obtained from the apolar fraction by fractionation over a silica column using hexane as eluent following the procedures reported by Belt et al. (2007) and Massé et al. (2011). After removing the solvent with N_2 at 35 °C, elemental sulfur was removed using the TBA (Tetrabutylammonium) sulfite method (Jensen et al., 1977; Riis and Babel, 1999). The obtained hydrocarbon fraction was analyzed within an Agilent 7890A gas chomatograph (GC) fitted with 30 m fused silica Agilent J&C GC column (0.25 mm i.d., 0.25 µm film thickness), coupled to a Agilent 5975C Series mass selective detector (MSD). The oven temperature in the GC was initially programmed at 40 °C, then increased by 10 °C min^{-1} up to 320 °C where it was held for 12 min. Spectra were then collected using the Agilent MS-Chemstation software. Individual HBIs were identified on the basis of comparison between their GC retention times and mass spectra with those of previously authenticated HBIs (e.g. Johns et al., 1999) and peaks of the two compounds were integrated using the Mass Hunter software. Values are expressed as concentration relative to the internal standards.

3.2.4 Diatoms

Diatom distribution and abundance in core JPC-10 was defined at a centennial scale resolution using the Crosta and Koç (2007) counting convention. Details regarding slide preparation and diatom identification are described in Crosta et al. (2004). Although the abundance of each diatom species was estimated as a percentage (%) of the *Chaetoceros*-free diatom assemblage, the total diatom abundance, *Chaetoceros*

CPD
9, 1–41, 2013

resting spores (CRS) and non-CRS assemblage absolute abundance were expressed as $Mv\,g^{-1}$ (millions of valves per gram of sediment). Species recording less than 1 % in every given sample were removed to decrease the effect of noise in the dataset, with the exception of several benthic species, which were grouped in a special benthic group. *Eucampia* specific counts, evaluating the relative abundances of the *Eucampia antarctica* var. *recta* ("polar" variety) versus *Eucampia antarctica* var. *antarctica* ("sub-polar" variety) and terminal versus intercalary valves were completed by counting 100 specimens per slide if abundance permitted, or by counting all specimens on a slide.

Here, we selected a number of diatom indicator species and groups of indicator species that reflect specific environments. In the Antarctic Peninsula, diatom species distribution follows a well-marked latitudinal gradient. CRS mostly develop in the northern part of the Antarctic Peninsula (Buffen et al., 2007; Pike et al., 2008), where the area has a longer ice-free season, and usually bloom during periods of most intense water column stratification (Crosta et al., 2007, 2008; Denis et al., 2006; Leventer et al., 1996). CRS are usually associated with high productivity (Crosta et al., 2007, 2008; Denis et al., 2006; Leventer et al., 1996, 2002) and constitute most of the preserved diatom species found in the JPC-10 sediments accounting for more than 90 % of the total diatom species. The dominant CRS exerts a strong control on diatom absolute abundance. We therefore distinguished the total diatom abundance with and without CRS. We performed CRS-free counts in order to insure that potentially important variations in the relative abundance of more minor diatom indicator species were not dampened by the overwhelming presence of CRS (e.g. Allen et al., 2005).

Other environmentally diagnostic and numerically abundant diatom species include cold variety of *Thalassiosira antarctica* which grows at the sea ice edge when the duration of seasonal sea ice is greatest (Buffen et al., 2007; Pike et al., 2009). *Fragilariopsis curta*, combined here with the very similar species *Fragilariopsis cylindrus*, is found close to sea ice (Buffen et al., 2007; Pike et al., 2008) and is used to reflect sea ice distribution. This ecological association has been widely applied by a number of authors (Crosta et al., 1998; Gersonde and Zielinski, 2000; Leventer, 1998; Gersonde

CPD
9, 1–41, 2013

et al., 2005; Allen et al., 2011; Collins et al., 2012). Currently, both *F. curta* and *F. cylindrus* are found to be more abundant in the southern WAP (Pike et al., 2008). *Eucampia Antarctica*, also common in JPC-10, has been documented to occur as two varieties, termed "sub-polar" and "polar" that are distinguished by valve symmetry (Fryxell, 1989; Fryxell and Prasad, 1990), and generally occur either north or south, respectively, of the Antarctic Convergence Zone. In addition, a paleoenvironmental proxy based on the ratio of terminal to intercalary valves of *Eucampia* has been used to record oscillations of winter sea ice (Kaczmarska et al., 1993; Whitehead et al., 2005). The abundance of *Fragilariopsis kerguelensis* and *Thalassiosira lentiginosa*, which presently reside off shore, and share a close relationship with the ACC, are used as indicators of open ocean conditions (Crosta et al., 2004), and might highlight summer sea-surface temperatures (Crosta et al., 2007). Finally, the sea ice related diatom group is compared to the so-called benthic group (composed of *Amphora*, *Cocconeis* sp., *Gomphonema*, *Licmophora* and *Navicula* sp.) which include cryophilic diatoms that live in near-coastal sea ice, and are commonly found during spring and summer blooms (Krebs, 1983).

4 Results

In JPC-10, the Holocene TEX_{86}^{L}-derived temperature record (0–200 water depth) reaches its maximum ($> \pm 3\,^{\circ}C$) at the bottom of the core, ~ 9000 yr BP (Fig. 3b). Following this peak, temperatures decreased to ~ +1.5 °C, until ~ 7000 yr BP, when a stepwise decrease occurred, followed by a declining trend. From ~ 7000 to 4200 yr BP, temperatures declined slightly from +1.6 to +0.7 °C, before experiencing a slowdown between ~ 4200 and 3000 yr BP and a second cooling phase, reaching a low (~ +0.3 °C) at ~ 3000 yr BP. Although the last 3000 yr BP were characterized by variable temperatures with a mean of +1.0 °C, the temperature record exhibited a peak at ~ 1000 yr BP, with values close to +2.5 °C. In comparison, our TEX_{86}^{L} record from ODP Site 1098 Hole B covering the last 12 000 yr BP revealed a temperature range from +3 °C to +0.3 °C (Fig. 4a). Although the temporal resolution of our ODP Site 1098 record is relatively low,

CPD
9, 1–41, 2013

the general trends of both records (JPC-10 and ODP Site 1098) are in good agreement (Fig. 4b), both in terms of overall temperature range and in highlighting the abrupt decrease in temperature from ~9000 to 8200 yr BP.

BIT values varied between 0.01 and 0.02 for both marine records (Fig. 4c). The low BIT values indicated that the input of soil organic matter (Hopmans et al., 2004) to our core sites was very low and, thus, did not influence our TEX_{86}^{L} record (cf. Weijers et al., 2006). The present-day vertical temperature profile in the study area shows a surface mixed layer (~30 m) with an average annual mean temperature of −0.2 °C and a 0–200 m water depth layer with an annual mean temperature of around +0.3 °C (Levitus and Boyer, 1994). Hence, the estimated temperatures of the upper most sediments analyzed (+1.2 °C for JPC-10 and +1.0 °C for ODP1098) are well above the regional freezing point of seawater (−1.7 °C, Martinson et al., 2008) and are only +1.0 °C warmer than the annual mean temperature of the 0–200 m water layer. Nevertheless, care has to be taken in interpreting the absolute values of TEX_{86}^{L}-derived reconstructions due to the relatively large calibration error (± 2.8 °C) Relative changes in TEX_{86}^{L}-derived temperature can be viewed with more confidence.

The HBI record (the ratio of D/T) is characterized by a two-step increase. Prior to ~7000 yr BP the ratio is uniformly low, close to 0, before increasing to values of 1–2 throughout the period of mid-Holocene cooling (Fig. 3). The ratio showed lower and more stable values (< 1) prior to and during the late Holocene (3700 to 1500 yr BP), before increasing again to higher values and a peak > 5 around 1000 yr BP, its highest values on average over the last 1200 yr BP. The mid-Holocene cooling and late Holocene patterns resemble each other (increasing from low to high values), albeit with greater D/T ratios during the late Holocene.

The total diatom and CRS absolute abundance evolved similarly over the last 9000 yr (Fig. 3). While the early Holocene warmth corresponded to low diatom and CRS abundance, around 200 $Mv\,g^{-1}$, the mid-Holocene cooling was represented by the highest diatom abundance with two peaks of 1200 and 900 $Mv\,g^{-1}$ at around 4800 and 4000 yr BP, respectively. The Late Holocene was marked by a decline in total diatom

CPD
9, 1–41, 2013

abundance with values close to those found prior to 7000 yr BP. Absolute abundance of diatoms other than *Chaetoceros* (Non-CRS assemblage data) increased from 20–40 Mv g^{-1} from 7000 yr BP, which is consistent with the total diatom abundance data, but then remained relatively high until the most recent part of the record (Figs. 3 and 5). CRS represent 80–90 % of the total abundance during the early Holocene, and increased slightly to 90–95 % during the mid-Holocene, prior to declining to ~ 70 % of the total abundance since 3000 yr (Fig. 5). The trend of *F. curta* and *F. cylindrus* showed a similar profile with low values, less than 10 % of the non-CRS total abundance, before 7000 yr BP, a net increase towards higher values during the mid-Holocene, reaching nearly 50 % at 5500 yr, followed by a decrease to values around 10–20 % over the last 1000 yr BP. In comparison, the cold variety of *T. antarctica* exhibited an overall increasing trend throughout the Holocene, rising from 2 to 12 %. *T. antarctica* relative abundance decreased slightly at around 3000 yr BP before experiencing a strong increase over the last 3000 yr BP. In contrast, *E. antarctica* was a significant component of the non-CRS total abundance between 9000 and 6000 yr BP (20–40 %) with a dominance of the sub-polar variety of the species, but then declined sharply at 6000 yr BP, representing a minor component throughout the remainder of the Holocene (mean 3.6 %). This decline was accompanied by the switch to a polar form of the species. In addition, the ratio of terminal/intercalary *Eucampia* valves was uniformly low until 6000 yr BP and then became higher and more variable. *F. kerguelensis* and *T. lentiginosa* occurred in relatively high abundances (20–30 %) before 7000 yr BP and progressively declined towards lower values, ranging between 10–20 %, over the course of the Holocene. This trend is opposite to the benthic group record, which revealed the lowest abundance during the early Holocene warmth, less than 3 %, before increasing to > 3 % from ~ 7000 to 4000 yr BP and declining thereafter.

CPD
9, 1–41, 2013

5 Discussion

5.1 Local comparison of TEX_{86}^{L} records in the WAP

Our new TEX_{86}^{L} records from JPC-10 and ODP Site 1098 Hole B (Fig. 4b) show a consistent picture of temperature variation in Palmer Deep Basin. However, our results give different temperature estimates in terms of amplitude and variations to the TEX_{86}-SST values published by Shevenell et al. (2011) (Fig. 4a). These differences are firstly due to the different indices used (TEX_{86}^{L} in our study and TEX_{86} in the study of Shevenell et al., 2011) as well as the different calibrations. We used the more extensive core-top data set of Kim et al. (2010) for our study, which contains far more data points from polar oceans than the calibration established by Kim et al. (2008) and used in Shevenell et al. (2011). Furthermore, we did not calibrate the TEX_{86} index against sea-surface temperature but the mean temperature integrated over the 0–200 m water depth range as outlined in Kim et al. (2012). Importantly, our ODP Site 1098 TEX_{86}^{L} record is fully consistent with the one from JPC-10 (Fig. 4b), thus suggesting that they represent a regional record of temperature variability.

5.2 The Holocene climate in the WAP

5.2.1 The early Holocene

Between ~10 000 and 7000 yr BP, TEX_{86}^{L}-derived temperatures were warmer than those during the mid and late Holocene (Figs. 3 and 4). With the exception of a cooling event centered ~8200 yr BP, which might be related to a global cooling phenomenon (Barber et al., 1999; Ellison et al., 2006; Morril and Jacobsen, 2005; Rohling and Pälike, 2005), temperatures varied from 1 °C to 3 °C, which is similar to modern observations under a warming climate (Martinson et al., 2008). Warm upper ocean temperatures are supported by the uniformly low relative abundance of the colder variety of *T. antarctica* (T1 variety) between 9000 and 7000 yr BP (Fig. 5). These relatively warm temperatures

CPD
9, 1–41, 2013

were probably accompanied by reduced seasonal sea ice presence as illustrated by the very low D/T ratio (< 03) (Fig. 3), the low relative abundances of diatoms groups associated with sea ice, including *F. curta* and *F. cylindrus*, the benthic diatom group, and the low ratio of terminal/intercalary *Eucampia* valves. The resulting prolonged open ocean conditions likely allowed for glacial melt and thus the production of stratification-related diatom species, such as *E. antarctica* and CRS, and open ocean species such as *F. kerguelensis* and *T. lentiginosa* (Fig. 5).

The early Holocene warm period (~ 12 000–7000 yr BP) has been recorded throughout the AP from both marine (Allen et al., 2010; Heroy et al., 2008; Sjunneskog and Taylor, 2002; Taylor et al., 2001; Taylor and Sjunneskog, 2002) and ice core records (Mulvaney et al., 2012), which report warmer conditions and/or weaker sea ice presence than today. High temperatures in our reconstructed record coincided with maximum annual and spring insolation since the onset of the Holocene (Fig. 3). Warmer-than-modern winter and spring conditions would have limited sea ice persistence and prolonged the local sea ice-free season. Given the link between insolation and sea ice, we infer that the latter likely retreated early in the spring and advanced late in the autumn during the early Holocene warmth, as supported by diatom assemblages. This would be consistent with warmer summer temperatures, estimated from model simulations to be slightly higher (0.5 °C) than today (Renssen et al., 2005), and the reconstructed atmospheric temperatures about +1 °C warmer than present days (Mulvaney et al., 2012).

A longer and warmer summer season, alongside a weaker sea ice presence, would have also likely favored the southward migration of the Westerlies as previously hypothesized (Shevenell et al., 2011). The southward migration of the Westerlies might have in turn increased the upwelling of warm UCDW and its transport onto the shelf, thus leading to higher ocean temperatures of between 1 and 2 °C. In addition, increased wind-driven coastal upwelling along with the reduced amount of near-shore sea ice cover might have enhanced the transport of nutrient-rich waters to the surface and hence allowed the renewal of the nutrient pool in the euphotic zone. Long seasonal periods of

CPD
9, 1–41, 2013

stratified conditions, followed by strong upwelling activity probably contributed in concert to stimulate diatom blooms during the early Holocene warmth along the WAP as recorded for instance here, in the Palmer Deep Basin.

5.2.2 The mid-Holocene

From ~7000 to 3000 yr BP, the TEX_{86}^{L}-derived temperature record indicated a slow cooling from +2 to +0.5 °C. This trend parallels decreasing annual and spring insolation, and increasing summer insolation (Renssen et al., 2005). The transition to a colder upper water column was also reflected in the overall increase in the relative abundance of *T. antarctica* T1 species at this time. This period of transition was concomitant with a pronounced increase in the D/T ratio (up to 2) (Fig. 3), suggesting an increasing seasonal presence of spring sea ice. The increasing abundance of diatoms species diagnostic of sea ice presence (*F. curta* and *F. cyclindrus*, *Eucampia* and the benthic diatom group) further support this scenario (Fig. 5) and suggest that regional sea ice persisted for longer throughout the year between ~7000 and 4200 yr BP. Reduced open ocean conditions are supported further by the decreasing abundance of open ocean diatom indicators, *F. kerguelensis* and *T. lentiginosa*. Proximity to a seasonally retreating sea ice edge likely promoted conditions conducive to CRS growth, also observed by Sjunneskog and Taylor (2002) in the Palmer Deep, through increased periods of sea ice melt-induced upper water column stratification. The strongly stratified conditions associated with an extended sea ice season generated higher productivity than permanently open ocean conditions as reflected in the total diatom abundance record. The mid-Holocene cooling ended with a shift in all proxy (for instance, increasing TEX_{86}^{L}-derived temperatures and D/T ratio, and decreasing total diatom abundance) records between ~4200 and 3000 yr BP.

During the mid-Holocene period, the reconstructed environmental conditions along the WAP do not show any clear homogenous picture of a regional climatic pattern (Allen et al., 2010; Domack et al., 2001; Heroy et al., 2008; Ishman and Sperling, 2002; Taylor and Sjunneskog, 2002; Taylor et al., 2001; Yoon et al., 2002). Overall,

CPD
9, 1–41, 2013

our TEX_{86}^{L}-derived temperature record points to a gradual cooling trend during the mid-Holocene, probably as the result of colder annual atmospheric temperatures and shorter summer duration associated with colder and longer winter and spring seasons, in turn driven by decreasing winter and spring insolation (Fig. 3) It is therefore likely that decreasing insolation in the winter and spring resulted in the development of a more extensive sea ice season which restricted the duration of the summer season, despite increasing summer insolation. This interpretation is supported by modeled temperatures that indicate a relatively continuous cooling trend of the annual and spring temperatures of 1 and 2 °C, respectively, over West Antarctica between ~ 9000 yr BP and today (Renssen et al., 2005). This is also consistent with recently reconstructed atmospheric temperatures that show a similar profile during this time interval (Mulvaney et al., 2012).

During the mid-Holocene, sea ice probably retreated later in the spring and advanced earlier in the autumn than previous Holocene periods. The melting of extensive sea ice would have led to stronger stratification of the water column, likely favoring the growth of *Chaetoceros* species and enhancing overall primary productivity in the Palmer Deep basin. A similar increase in marine primary productivity was also reported in Lallemand Fjord (Taylor et al., 2001; Shevenell et al., 1996) and Marguerite Bay (Allen et al., 2010), although a decrease in CRS was reported for the former region. This could be related to the more southerly and coastal location of Lallemand Fjord, which may have contributed to stronger sea ice development that prevented the occurrence of large blooms of *Chaetoceros*. The extension of sea ice might have displaced the Westerlies northward, and the resulting reduced upwelling of UCDW might have led to a diminished transport of warm waters masses over the WAP shelf. Due to the longer seasonal persistence of sea ice along the shore and the reduced effects of the katabatic and synoptic winds, decreased coastal upwelling would have acted to limit the intrusion of warm waters to the surface, thus further decreasing temperatures.

CPD
9, 1–41, 2013

5.2.3 The late Holocene

The late Holocene was characterized by more variable TEX_{86}^{L}-derived temperatures, ranging between ±0.3 °C and 2.5 °C with the maximum reached at ∼1000 yr BP (Fig. 3). The *T. antarctica* T1 data also exhibit large swings, superimposed onto a general cooling trend as suggested by the overall increased average relative abundance of this colder water variety of *T. antarctica* (Fig. 5). The most abrupt shift in the ratio of D/T (up to 5) occurred at ∼2000 yr BP and implies that the late Holocene corresponded to a period of increased sea ice presence (Fig. 3). This is further supported by the continued high relative abundances of *F. curta* and *F. cylindrus*, as well as the benthic diatom group (Fig. 5). Conversely, the typically open ocean diatoms *F. kerguelensis* and *T. lentiginosa* reached their lowest abundance during this period indicating the shortest seasonal open ocean period throughout the Holocene. Furthermore, the CRS and the total diatom abundance declined during this period (Fig. 5) a trend unexpected considering the extent of upper water column stratification anticipated from the melting of such extensive sea ice cover. It has been shown that high surface water stratification generally leads to high productivity and, especially, high CRS production in the western Weddell Sea (Buffen et al., 2007). It is therefore possible that decreased water column stratification due to wind action reduced diatom abundance during this period as already evidenced in Bransfield Strait (Heroy et al., 2008).

The late Holocene (∼3000–600 yr BP) has been extensively described as a period of drastic environmental conditions changes in the AP that might be related to ocean cooling (for example, Allen et al., 2010; Björk et al., 1996a; Domack and McClennen, 1996; Heroy et al., 2008; Taylor et al., 2001; Taylor and Sjunneskog, 2002; Sjunneskog and Taylor, 2002) and atmospheric cooling (Mulvaney et al., 2012). During this period, the HBI record from JPC-10 suggests the greatest sea ice duration since the onset of the Holocene, which is consistent with previous findings further south (Allen et al., 2010) and north (Heroy et al., 2008). Annual and spring insolation at 65° S reach a minimum during this period of time, while summer insolation attains a Holocene maximum.

CPD
9, 1–41, 2013

We suggest that despite maximum summer insolation, summer duration was probably its shortest since the early Holocene and colder and longer winter and spring seasons would have likely promoted longer sea ice seasons, thus supporting previous work in East Antarctica (Pike et al., 2009).

In contrast to the icy environment implied by diatom assemblage and HBI data, the JPC-10 TEX-derived temperature record suggests relatively warmer conditions during the ice-free months, and thus a rather rapid transition from a cold spring to a warm summer. A regime shift of this nature would have likely hindered a long, stable period of stratification and curtailed the associated growing season, as evidenced by the decreasing trends in CRS and total diatom abundance. A shorter growing season in the WAP is further supported by similar results from Marguerite Bay (Allen et al., 2010). However, we believe it is unlikely that variations in seasonal insolation alone were responsible for the climatic changes observed over the WAP during the mid to late Holocene. For example, despite low and relatively stable annual and spring insolation since 2000 yr BP, HBI and sea ice-related diatom records continued to show large amplitude changes throughout this period. Furthermore, the simulated atmospheric temperatures indicate summer cooling and relatively stable winter and spring conditions (Renssen et al., 2005) which is consistent with the atmospheric cooling trend reconstructed in the eastern Antarctic Peninsula (Mulvaney et al., 2012), while our TEX^{L}_{86}-derived temperatures illustrate a slight annual warming (+1 °C) and the D/T ratio and diatom assemblages report winter and spring cooling. An additional explanation is therefore required.

5.2.4 The influence of ENSO in the WAP

An intriguing aspect of the D/T ratio from JPC-10 is the increased range of variability from ~4500 to 4000 yr BP and again from ~1200 yr BP to the top of the core. The applicability of this proxy as an indicator of sea ice suggests greater variability of sea ice extent during those time intervals, and in contrast a lesser variability during the periods ~7000–4500 yr BP, ~4000–1200 yr BP and ~9000 to 7000 yr BP, when the D/T ratio

CPD
9, 1–41, 2013

was less variable and uniformly low, respectively. The question is not only what caused the changes in the average D/T ratio, but also the cause of higher frequency variability.

Similar high climate variability has been found at low latitudes since ~5000 yr BP and related to the intensification of centennial scale ENSO activity (Chazen et al., 2009; Conroy et al., 2008; Moy et al., 2002). Recent work additionally demonstrates the impact of ENSO on Antarctic climate (Kwok and Comiso, 2002; Turner et al., 2004; Yuan and Martinson, 2000; Shevenell et al., 2011). Strength and frequency of ENSO vary in line with changes in east-west temperature and pressure gradients along the equatorial Pacific. During El Niño events, greater heat flux in the eastern Pacific propagates to the Antarctic coastal regions in the Pacific Ocean sector through Rossby wave trains, resulting in warmer conditions and reduced sea ice (Yuan et al., 2004). Conversely, during La Niña events, when temperatures are much lower in the eastern than western equatorial Pacific, heat flux is diminished and colder conditions are correlated with more sea ice in the Pacific Ocean sector of Antarctica (Yuan et al., 2004). Temperatures and sea ice around Antarctica seem to be more sensitive to the cold La Niña events than the warm El Niño events and respond with greater amplitude to the former (Yuan and Martinson, 2001). However, these two climatic states also induce a shift in the Westerlies, with the circumpolar wind belt transposed further south during La Niña events, which would in turn cause an increase in the upwelling of warm UCDW, thereafter propagating the El Niño and La Niña signal into the warming WAP surface waters (Martinson et al., 2008; Willmott et al., 2010). Steig et al. (2012) also highlight the potential importance of forcing from the Tropical Pacific in regulating the flow of UCDW onto the West Antarctic continental shelf.

Here we compare the sea ice-related HBI data from the Palmer Deep, with a suite of ENSO proxy records, including those of Conroy et al. (2008) from the Galapagos, Moy et al. (2002) from the Ecuadorian Andes and Makou et al. (2011) from ODP Site 1228D on the Peruvian continental margin (Fig. 6). All the records document minimum frequency of ENSO events in the early Holocene, coincident with the time of the most uniform, and lowest D/T ratios, indicative of uniformly reduced sea ice cover. The

CPD
9, 1–41, 2013

peak to peak correlation between the ENSO and HBI data is not as clear for the remainder of the record but generally higher D/T ratios are in phase with greater ENSO activity (Fig. 6). From ~7000 to 4500 yr BP sea ice extent and variability demonstrate increasing trends, with mid-Holocene peaks in D/T ratios and variability observed between ~4500 to 4000 yr BP. The ENSO records from Conroy et al. (2006) and Moy et al. (2002) similarly record increasing variability and frequency of ENSO at this time. Between ~4000 and 2100 yr BP, no strong sea ice variations are recorded in phase with low ENSO activity recorded at the Equator (e.g. Moy et al., 2002) and Peru margin (Makou et al., 2011). However, a phase of increasing ENSO frequency was conversely recorded in the Galapagos area (Conroy et al., 2008). Finally, over the last 2100 yr BP, increasing ENSO frequency concomitant with the appearance of stronger La Niña events (Makou et al., 2011) is coincident with the greatest variability in the D/T ratio. Given these data, we suggest, in line with Shevenell et al. (2011), that ENSO variability may have been one of the main drivers of the sea ice seasonal cycle at centennial to millennial timescales in the WAP, with increasing influence in the later Holocene. In particular, we note the data of Das and Alley (2008) that documents increased melt frequency at Siple Dome through the late Holocene; they suggest the role of increased storm activity and the inland movement of maritime warm and moist air, perhaps related to ENSO variability. However, considering the lack of correlation between our sea ice data and ENSO variability between ~4000 and 2100 yr BP, we further propose that other factors also linked to the Antarctic Dipole (the Southern Annular Mode) and other low-latitude climate oscillations (e.g. Indian or Atlantic Ocean Dipole), may also play a role in controlling sea ice in the Antarctic Peninsula. Clearly, the role of ENSO and tropical forcing of Southern Ocean climate needs greater investigation.

Our results indicate that sea ice persisted longer during phases of stronger La Niña events (the last 2100 yr) while upper ocean temperatures became higher as shown by the increasing D/T ratio TEX^{L}_{86}-derived temperature from JPC-10, respectively. During La Niña events, it is likely that a southernmost position of the Westerlies would be accompanied by a reinforcement of the upwelling of warm waters, which

CPD
9, 1–41, 2013

would in turn affect the WAP surface waters and preclude thick and long seasonal sea ice cover (Martinson et al., 2008; Willmott et al., 2010). The HBI record is not consistent with such a scenario, suggesting instead that the pronounced presence of sea ice coincided with our reconstructed high TEX_{86}^{L}-derived temperatures. In contrast, increasing abundance of cold water diatom species (e.g. *T. antarctica*) indicated that colder conditions characterized the winter, potentially promoting pronounced sea ice extent. Such a pattern can be validated if we reasonably suppose that the increasing ENSO frequency associated with more La Niña events (Makou et al., 2011) might have led to an increase in seasonal variability with greater amplitude between the warm summer and cold winter seasons. Given the low annual insolation, higher ENSO frequency and stronger La Niña events during the past 2000 yr BP, the WAP climatic variability might have been governed by an alternation of "extremely" warm and cold temperatures, which would explain the contrasting relatively high temperatures and enhanced sea ice cover recorded in JPC-10 and reported elsewhere (Denis et al., 2010). Despite increased sea ice during winter and late spring, warmer temperatures and stronger wind activity during the summer could have led to more rapid sea ice retreat and a stronger upwelling of warm waters, which together may prevent long periods of the stratified conditions that are conducive to diatom and particularly CRS blooms.

6 Summary and conclusions

In this study, we examined the WAP climate variability over the last 9000 yr BP using a suite of proxies, including diatom assemblage data and biomarkers, to reconstruct the variations in sea ice temperature and diatom productivity, from a core located in the Palmer Deep Basin. Overall, the data document a cooling trend and gradually increasing sea ice extent throughout the Holocene, potentially in response to decreasing annual and spring insolation. This lends support to recent suggestions that decreasing regional annual and seasonal mean insolation were the main drivers of temperature

CPD
9, 1–41, 2013

and sea ice changes occurring in the Southern Hemisphere over the last climatic cycle (Huybers and Denton, 2009).

Early Holocene warmth corresponded to a longer sea ice-free season with warm upper ocean temperatures probably linked to the upwelling of warm UCDW. Coeval with declining insolation, the midHolocene was in contrast characterized by a cooling trend, longer seasonal sea ice duration and extensive marginal ice zone conditions, which in turn resulted in maximum regional productivity. During the late Holocene, particularly over the last 2000 yr BP, the WAP experienced a major climatic step, and was characterized by an exceptionally long sea ice season which persisted until late in spring season.

During the Holocene, we suggest the role of low-latitude climate forcing on sea ice and local oceanic conditions. When comparing lower latitude proxy records of ENSO frequency with our multi-proxy data, we suggest that increasing ENSO frequency and decreasing insolation might have together, amplified the seasonal contrast between a warm summer and a cold winter. An exception is made for the period between 4000 and 2100 yr BP when neither HBIs nor TEX_{86}^{L} records showed a strong correspondence with ENSO variability. We propose the operation of additional influencing factors related to the West and East Antarctic dipoles (SAM), northern high latitudes (e.g. AMOC) and/or other tropical/subtropical climate influences (e.g. Indian Ocean Dipole) expressed through oceanic and atmospheric teleconnections during this period. Thus, further high-resolution investigations around Antarctica, in particularly in the eastern sector, are required for a better understanding of the processes controlling WAP climate during this period of time.

Acknowledgements. We greatly thank Marie-Hélène Taphanel for technical assistance. We also acknowledge funding from the French ANR CLIMICE, ESF PolarClimate HOLOCLIP 625, and ERC ICEPROXY 203441 as well as the Netherlands Organisation of Scientific Research (NWO) through a VICI grant to Stefan Schouten.

CPD
9, 1–41, 2013

The publication of this article is financed by CNRS-INSU.

References

Allen, C. S., Pike, J., Pudsey, C. J., and Leventer, A.: Submillennial variations in ocean conditions during deglaciation based on diatom assemblages from the southwest Atlantic, Paleoceanography, 20, PA2012, doi:10.1029/2004PA001055, 2005.

Allen, C. S., Oakes-Fretwell, L., Anderson, J. B., and Hodgson, D. A.: A record of Holocene glacial and oceanographic variability in Neny Fjord, Antarctic Peninsula, Holocene, 20, 551–564, 2010.

Alonso-Sáez, L., Waller, A. S., Mende, D. R., Bakker, K., Farnelid, H., Yager, P. L., Lovejoy, C., Tremblay, J.-É., Potvin, M., Heinrich, F., Estrada, M., Riemann, M., L., Bork, P., Pedrós-Alió, C., and Bertilsson, S.: Role for urea in nitrification by polar marine Archaea, P. Natl. Acad. Sci. USA, 109, 17989–17994, doi:10.1073/pnas.1201914109, 2012.

Anderson, R. F., Ali, S., Bradtmiller, L. I., Nielsen, S. H. H., Fleisher, M. Q., Anderson, B. E., and Burckle, L. H.: Wind-driven upwelling in the Southern Ocean and the deglacial rise in atmospheric CO_2, Science, 323, 1443–1448, 2009.

Annett, A. L., Carson, D. S., Crosta, X., Clarke, A., and Ganeshram, R. S.: Seasonal progression of diatom assemblages in surface waters of Ryder Bay, Antarctica, Polar Biol., 33, 13–29, 2010.

Barbara, L., Crosta, X., Massé, G., and Ther, O.: Deglacial envrionments in eastern Prydz Bay, East Antarctica, Quaternary Sci. Rev., 29, 2731–2740, 2010.

Barber, D. C., Dyke, A., Hillaire-Marcel, C., Jennings, A. E., Andrews, J. T., Kerwin, M. W., Bilodeau, G., McNeely, R., Southon, J., Morehead, M. D., and Gagnon, J.-M.: Forcing of the cold event of 8200 years ago by catastrophic drainage of Laurentide lakes, Nature, 400, 344–348, 1999.

CPD
9, 1–41, 2013

Belt, S. T., Allard, W. G., Massé, G., Robert, J. M., and Rowland, S. J.: Highly branched isoprenoids (HBIs): identification of the most common and abundant sedimentary isomers, Geochim. Cosmochim. Ac., 64, 3839–3851, 2000.

Belt, S. T., Massé, G., Rowland, S. J., Poulin, M., Michel, C., and LeBlanc, B.: A novel chemical fossil of palaeo sea ice: IP25, Org. Geochem., 38, 16–27, 2007.

Bentley, M. J., Hodgson, D. A., Smith, J. A., Cofaigh, C. Ó., Domack, E. W., Larter, R. D., Roberts, S. J., Brachfeld, S., Leventer, A., Hjort, C., Hillenbrand, C.-D., and Evans, J.: Mechanisms of Holocene palaeoenvironmental change in the Antarctic Peninsula region, Holocene, 19, 51–69, 2009.

Bentley, M. J., Johnson, J. S., Hodgson, D. A., Dunai, T., Freeman, S. P. H. T., and Cofaigh, C. O.: Rapid deglaciation of Marguerite Bay, western Antarctic Peninsula in the Early Holocene, Quaternary Sci. Rev., 30, 3338–3349, 2011.

Berger, A. and Loutre, M. F.: Insolation values for the climate of the last 10 million years, Quaternary Sci. Rev., 10, 297–317, 1991.

Buffen, A., Leventer, A., Rubin, A., and Hutchins, T.: Diatom assemblages in surface sediments of the northwestern Weddell Sea, Antarctic Peninsula, Mar. Micropaleontol., 62, 7–30, 2007.

Burckle, L. H.: Ecology and paleoecology of the marine diatom eucampia-antarctica (castr) mangin, Mar. Micropaleontol., 9, 77–86, 1984.

Collins, L. G., Pike, J., Allen, C. S., and Hodgson, D. A.: High resolution reconstruction of Southwest Atlantic sea-ice and its role in the carbon cycle during Marine Isotope Stages 3 and 2, Paleoceanography, 27, PA3217, doi:10.1029/2011PA002264, 2012.

Conroy, J. L., Overpeck, J. T., Cole, J. E., Shanahan, T. M., and Steinitz-Kannan, M.: Holocene changes in eastern tropical Pacific climate inferred from a Galápagos lake sediment record, Quaternary Sci. Rev., 27, 1166–1180, 2008.

Cowie, R. O. M., Maas, E. W., and Ryan, K. G.: Archaeal diversity revealed in Antarctic sea ice, Antarct. Sci., 23, 531–536, 2011.

Crosta, X. and Koç, N.: Diatoms: from micropaleontology to isotope geochemistry, in: Developments in Marine Geology, Elsevier, 327–369, 2007.

Crosta, X., Pichon, J. J., and Burckle, L. H.: Application of modern analog technique to marine Antarctic diatoms: reconstruction of maximum sea-ice extent at the Last Glacial Maximum, Paleoceanography, 13, 284–297, 1998.

CPD
9, 1–41, 2013

Crosta, X., Sturm, A., Armand, L., and Pichon, J. J.: Late Quaternary sea ice history in the Indian sector of the Southern Ocean as recorded by diatom assemblages, Mar. Micropaleontol., 50, 209–223, 2004.
Crosta, X., Debret, M., Denis, D., Courty, M. A., and Ther, O.: Holocene long- and short-term climate changes off Adelie Land, East Antarctica, Geochem. Geophy. Geosy., 8, 1–15, 2007.
Crosta, X., Denis, D., and Ther, O.: Sea ice seasonality during the Holocene, Adélie Land, East Antarctica, Mar. Micropaleontol., 66, 222–232, 2008.
Das, S., Alley, R. B.: Rise in frequency of surface melting at Siple Dome through the Holocene: evidence for increasing marine influence on the climate of West Antarctica, J. Geophys. Res.-Atmos., 113, D02112, doi:10.1029/2007JD008790, 2008.
Denis, D., Crosta, X., Zaragosi, S., Romero, O., Martin, B., and Mas, V.: Seasonal and subseasonal climate changes recorded in laminated diatom ooze sediments, Adelie Land, East Antarctica, Holocene, 16, 1137–1147, 2006.
Denis, D., Crosta, X., Barbara, L., Massé, G., Renssen, H., Ther, O., and Giraudeau, J.: Sea ice and wind variability during the Holocene in East Antarctica: insight on middle-high latitude coupling, Quaternary Sci. Rev., 29, 3709–3719, 2010.
Dierssen, H. M., Smith, R. C., and Vernet, M.: Glacial meltwater dynamics in coastal waters west of the Antarctic peninsula, P. Natl. Acad. Sci. USA, 99, 1790–1795, 2002.
Ding, Q., Steig, E. J., Battisti, D. S., and Küttel, M.: Winter warming in West Antarctica caused by central tropical Pacific warming, Nat. Geosci., 4, 398–403, doi:10.1038/ngeo1129, 2011
Doake, C. S. M. and Vaughan, D. G.: Rapid disintegration of the wordie ice shelf in response to atmospheric warming, Nature, 350, 328–330, 1991.
Domack, E. W. and McClennen, C. E.: Accumulation of glacial marine sediments in fjords of the Antarctic Peninsula and their use as late Holocene paleoenvironmental indicators, in: Foundations for ecosystem research west of the Antarctic Peninsula, Antarctic Research Series, vol 70, edited by: Ross, R., et al., American Geophysical Union, 135–154, 1996.
Domack, E., Leventer, A., Dunbar, R., Taylor, F., Brachfeld, S., and Sjunneskog, C.: Chronology of the Palmer Deep site, Antarctic Peninsula: a Holocene palaeoenvironmental reference for the circum-Antarctic, Holocene, 11, 1–9, 2001.
Ellison, C. R. W., Chapman, M. R., and Hall, I. R.: Surface and deep ocean interactions during the cold climate event 8200 years ago, Science, 312, 1929–1932, 2006.
Fryxell, G. A.: Marine phytoplankton at the Weddell Sea ice edge: seasonal changes at the specific level, Polar Biol., 10, 1–18, 1989.

CPD
9, 1–41, 2013

Fryxell, G. A. and Prasad, A. K. S. K.: *Eucampia antarctica* var. recta (Mangin) stat. nov. (Biddulphiaceae, Bacillariophyceae): life stages at the Weddell Sea ice edge, Phycologia, 29, 27–38, 1990.

Gersonde, R. and Zielinski, U.: The reconstruction of Late Quaternary Antarctic sea-ice distribution – the use of diatoms as a proxy for sea ice, Palaeogeogr. Palaeocl., 162, 263–286, 2000.

Gersonde, R., Crosta, X., Abelmann, A., and Armand, L.: Sea-surface temperature and sea ice distribution of the Southern Ocean at the EPILOG Last Glacial Maximum – a circum-Antarctic view based on siliceous microfossil records, Quaternary Sci. Rev., 24, 869–896, 2005.

Hammer, C. U., Claussen, H. B., and Langway Jr., C. C.: Electrical conductivity method (ECM) stratigraphic dating of the Byrd station ice core, Antarctica, Ann. Glaciol., 20, 115–120, 1994.

Heroy, D. C., Sjunneskog, C., and Anderson, J. B.: Holocene climate change in the Bransfield basin, Antarctic Peninsula: evidence from sediment and diatom analysis, Antarct. Sci., 20, 69–87, 2008.

Hjort, C., Bentley, M. J., and Ingólfsson, Ó.: Holocene and pre-Holocene temporary absence of the George VI Ice Shelf, Antarctic Peninsula, Antarct. Sci., 13, 296–301, 2001.

Hopmans, E. C., Schouten, S., Pancost, R. D., v. d. Meer, J., and Sinninghe Damsté, J. S.: Analysis of intact tetraether lipids in archaeal cell material and sediments using high performance liquid chromatography/atmospheric pressure ionization mass spectrometry, Rapid Commun. Mass Sp., 14, 585–589, 2000.

Huybers, P. and Denton, G.: Antarctic temperature at orbital timescales controlled by local summer duration, Nat. Geosci., 1, 787–792, 2008.

Ingólfsson, Ó., Hjort, C., and Humlum, O.: Glacial and climate history of the Antarctic Peninsula since the last glacial maximum, Arct. Antarct. Alp. Res., 35, 175–186, 2003.

Ishman, S. E. and Sperling, M. R.: Benthic foraminiferal record of Holocene deep-water evolution in the Palmer Deep, western Antarctic Peninsula, Geology, 30, 435–438, 2002.

Jensen, S., Renberg, L., and Reutergårdh, L.: Residue analysis of sediment and sewage sludge for organochlorines in the presence of elemental sulphur, Anal. Chem., 49, 316–318, 1977.

Johns, L., Wraige, E. J., Belt, S. T., Lewis, C. A., Massé, G., Robert, J.-M., and Rowland, S. J.: Identification of C25 Highly Branched Isoprenoid (HBI) Dienes in Antarctic sediments, sea-ice diatoms and laboratory cultures of diatoms, Org. Geochem., 30, 1471–1475, 1999.

CPD
9, 1–41, 2013

Johnson, J. S., Bentley, M. J., Roberts, S. J., Binnie, S. A., and Freeman, S. P. H. T.: Holocene deglacial history of the northeast Antarctic Peninsula – a review and new chronological constraints, Quaternary Sci. Rev., 30, 3791–3802, 2011.

Jouzel, J., Vaikmae, R., Petit, J.-R., Martin, M., Duclos, Y., Stievenard, M., Lorius, C., Toots, M., Melières, M.-A., Burckle, L. H., Barkov, N. I., and Kotlyakov, V. M.: The two-step shape and timing of the last deglaciation in Antarctica, Clim. Dynam., 11, 151–161, 1995.

Joughin, I. and Alley, R. B.: Stability of the West Antarctic ice sheet in a warming world, Nat. Geosci., 4, 506–513, 2011.

Kaczmarska, I., Barbrick, N. E., Ehrman, J. M., and Cant, G. P.: Eucampia Index as an indicator of the Late Pleistocene oscillations of the winter sea-ice extent at the ODP Leg 119 Site 745B at the Kerguelen Plateau, Hydrobiologia, 269/270, 103–112, 1993.

Kalanetra, K. M., Bano, N., and Hollibaugh, J. T.: Ammonia-oxidizing Archaea in the Arctic Ocean and Antarctic coastal waters, Environ. Microbiol., 11, 2434–2445, 2009.

Kim, J.-H., Schouten, S., Hopmans, E., Donner, B., and Sinninghe Damsté, J. S.: Global sediment core-top calibration of the TEX_{86} paleothermometer in the ocean, Geochim. Cosmochim. Ac., 72, 1154–1173, 2008.

Kim, J.-H., v. d. Meer, J., Schouten, S., Helmke, P., Wilmott, V., Sangiorgi, F., Koç, N., Hopmans, E. C., and Sinninghe Damsté, J. S.: New indices and calibrations derived from the distribution of creanarchaealisoprenoidtetraether lipids: implications for past sea surface temperature reconstructions, Geochim. Cosmochim. Ac., 74, 4639–4654, 2010.

Kim, J.-H., Crosta, X., Willmott, V., Renssen, H., Massé, G., Bonnin, J., Helmke, P., Schouten, S., and Sinninghe Damsté, J. S.: Increase in Late Holocene subsurface temperature variability in East Antarctica, Geophys. Res. Lett., 39, L06705, doi:10.1029/2012GL051157, 2012.

King, J.: Recent climate variability in the vicinity of the Antarctic Peninsula, Int. J. Climatol., 14, 357–369, 1994.

Klinck, J. M., Hofmann, E. E., Beardsley, R. C., Salihoglu, B., and Howard, S.: Watermass properties and circulation on the west Antarctic Peninsula Continental Shelf in Austral Fall and Winter 2001, Deep-Sea Res. Pt. II, 51, 1925–1946, 2004.

Krebs, W. N.: Ecology of neritic marine diatoms, Arthur Harbor, Antarctica, Micropaleontology, 29, 267–297, 1983.

Kwok, R. and Comiso, J. C.: Southern Ocean climate and sea ice anomalies associated with the Southern Oscillation, Am. Meteor. Soc., 15, 487–501, 2002.

CPD
9, 1–41, 2013

Leventer, A.: The fate of Antarctic "sea-ice diatoms" and their use as paleoenvironmental indicators, in: Antarctic sea ice biological processes, interactions and variability, Antarctic Res. Ser., Vol. 121–137, edited by: Lizotte, M. and Arrigo, K., Am. Geophys. Un.,, 1626–1644, 1998.

Leventer, A., Domack, E. W., Ishman, S. E., Brachfeld, S., McClennen, C. E., and Manley, P.: Productivity cycles of 200–300 years in the Antarctic Peninsula Region: understanding linkages among the sun, atmosphere, oceans, sea ice, and biota, Geol. Soc. Am. Bull., 108, 1626–1644, 1996.

Leventer, A., Domack, E., Barkoukis, A., McAndrews, B., and Murray, J.: Laminations from the Palmer Deep: A diatom-based interpretation, Paleoceanography, 17, 8002, doi:10.1029/2001PA000624, 2002.

Levitus, S., Antonov, J. I., Boyer, T. P., and Stephens, C.: Warming of the world ocean, Science, 287, 2225–2229, 2000.

Makou, M. C., Eglinton, T. I., Oppo, D. W., and Hughen, K. A.: Postglacial changes in El Niño and La Niña behavior, Geology, 38, 43–46, 2011.

Marinov, I., Gnanadesikan, A., Toggweiler, J. R., and Sarmiento, J. L.: The Southern Ocean biogeochemical divide, Nature, 441, 964–967, 2006.

Martinson, D. G., Stammerjohn, S. E., Iannuzzi, R. A., Smith, R. C., and Vernet, M.: Western Antarctic Peninsula physical oceanography and spatio-temporal variability, Deep-Sea Res. Pt. II, 55, 1964–1987, 2008.

Massé, G., Rowland, S. J., Sicre, M.-A., Jacob, J., Jansen, E., and Belt, S. T.: Abrupt climate changes for Iceland during the last millennium: evidence from high resolution sea ice reconstructions, Earth Planet. Sc. Lett., 269, 564–568, 2008.

Massé, G., Belt, S., Crosta, X., Schmidt, S., Snape, I., Thomas, D. N., and Rowland, S. J.: Highly branched isoprenoids as proxies for variable sea ice conditions in the Southern Ocean, Antarct. Sci., 23, 487–498, 2011.

Masson-Delmotte, V., Buiron, D., Ekaykin, A., Frezzotti, M., Gallé, H., Jouzel, J., Krinner, G., Landais, A., Motoyama, H., Oerter, H., Pol, K., Pollard, D., Ritz, C., Schlosser, E., Sime, L. C., Sodemann, H., Stenni, B., Uemura, R., and Vimeux, F.: A comparison of the present and last interglacial periods in six Antarctic ice cores, Clim. Past, 7, 397–423, doi:10.5194/cp-7-397-2011, 2011.

Matsumoto, G. I., Matsumoto, E., Sasaki, K., and Watanuki, K.: Geochemical features of organic matter in sediment cores from Lützow-Holm bay, Antarctica, in: Organic Matter: Pro-

CPD
9, 1–41, 2013

ductivity, Accumulation, and Preservation in Recent and Ancient Sediments, edited by: Whelan, J. K. and Farrington, J. W., Columbia University Press, New York, 142–175, 1992.
Moffat, C., Beardsley, R. C., Owens, B., and van Lipzig, N.: A first description of the Antarctic Peninsula Coastal Current, Deep-Sea Res. Pt. II, 55, 277–293, 2008.
Morill, C. and Jacobsen, R. M.: How widespread were climate anomalies 8200 years ago?, Geophys. Res. Lett., 32, L19701, doi:10.1029/2005GL023536, 2005.
Moy, C. M., Seltzer, G. O., Rodbell, D. T., and Anderson, D. M.: Variability of El Niño/Southern Oscillation activity at millennial timescales during the Holocene epoch, Nature, 420, 162–165, 2002.
Orsi, A. H., Smethie Jr., W. M., and Bullister, J. L.: On the total input of Antarctic waters to the deep ocean: a preliminary estimate from chlorofluorocarbon measurements, J. Geophys. Res., 107, 3122, doi:10.1029/2001JC000976, 2002.
Pike, J., Allen, C. S., Leventer, A., Stickley, C., and Pudsey, C. J.: Comparison of contemporary and fossil diatom assemblages from the western Antarctic Peninsula shelf, Mar. Micropaleontol., 67, 274–287, 2008.
Pike, J., Crosta, X., Maddison, E. J., Stickley, C. E., Denis, D., Barbara, L., Renssen, H., and Leventer, A.: Observations on the relationship between the Antarctic coastal diatoms *Thalassiosira antarctica* Comber and *Porosira glacialis* (Grunow) Jørgensen and sea ice concentrations during the Late Quaternary, Mar. Micropaleontol., 73, 14–25, 2009.
Renssen, H., Goosse, H., Fichefet, T., Masson-Delmotte, V., and Koc, N.: Holocene climate evolution in the high-latitude Southern Hemisphere simulated by a coupled atmosphere-sea ice-ocean-vegetation model, Holocene, 15, 951–964, 2005.
Rignot, E.: Changes in ice dynamics and mass balance of the Antarctic ice sheet, Philos. T. Roy. Soc., 364, 1637–1655, 2006.
Rintoul, S. R., Hughes, C. W., and Olbers, D.: The Antarctic circumpolar current system, in: Ocean Circulation and Climate. Observing and Modelling the Global Ocean, edited by: Siedler, G., Church, J., and Gould, J., Academic Press, 271–302, 2001.
Riis, V. and Babel, W.: Removal of sulfur interfering in the analysis of organochlorines by GC-ED, Analyst, 124, 1771–1773, 1999.
Robson, J. N. and Rowland, S. J.: Biodegradation of highly branched isoprenoid hydrocarbons: a possible explanation of sedimentary abundance, Org. Geochem., 13, 691–695, 1988.
Rohling, E. J. and Pälike, H.: Centennial-scale climate cooling with a sudden cold event around 8200 years ago, Nature, 434, 975–979, 2005.

CPD
9, 1–41, 2013

Rott, H., Skvarca, P., and Agler, T.: Rapid collapse of Northern Larsen Ice Shelf, Antarct. Sci., 271, 788–792, 1996.

Sarmiento, J. L., Gruber, N., Brzezinski, M. A., and Dunne, J. P.: High-latitude controls of thermocline nutrients and low latitude biological productivity, Nature, 427, 56–60, 2004.

Schouten, S., Hopmans, E. C., Schefuß, E., and Sinninghe Damsté, J. S.: Distributional variations in marine crenarchaeotal membrane lipids: a new organic proxy for reconstructing ancient sea water temperatures, Earth Planet. Sc. Lett., 204, 265–274, 2002.

Schouten, S., Huguet, C., Hopmans, E. C., Kienhuis, M., and Sinninghe Damsté, J. S.: Analytical methodology for TEX_{86} paleothermometry by high-performance liquid chromatography/atmospheric pressure chemical ionization-mass spectrometry, Anal. Chem., 79, 2940–2944, 2007.

Shevenell, A. E., Domack, E. W., and Kernan, G. M.: Record of Holocene palaeoclimate change along the Antarctic Peninsula: evidence from glacial marine sediments, Lallemand Fjord, Pap. Proc. Roy. Soc. Tasmania, 130, 55–64, 1996.

Shevenell, A. E., Ingalls, A. E., Domack, E. W., and Kelly, C.: Holocene Southern Ocean surface temperature variability west of the Antarctic Peninsula, Nature, 470, 250–254, 2011.

Sinninghe Damsté, J. S., Rijpstra, W. I. C., Coolen, M. J. L., Schouten, S., and Volkman, J. K.: Rapid sulfurisation of highly branched isoprenoid (HBI) alkenes in sulfidic Holocene sediments from Ellis Fjord, Antarctica, Org. Geochem. 38, 128–139, 2007.

Sjunneskog, C. and Taylor, F.: Postglacial marine diato record of the Palmer Deep, Antarctic Peninsula (ODP Leg 178, Site 1098), 1. Total diatom abundance, Paleoceanography, 17, 8003, doi:10.1029/2000PA000563, 2002.

Smith, D. A., Hofmann, E. E., Klinck, J. M., and Lascara, C. M.: Hydrography and circulation of the west Antarctic Peninsula continental shelf, Deep-Sea Res. Pt. I, 46, 925–949, 1999.

Stammerjohn, S. E. and Smith, R. C.: Spatial and temporal variability of western Antarctic Peninsula sea ice coverage, in: Foundations for ecological research west of the Antarctic Peninsula, Am. Geophys. Un., 81–104, 1996.

Stammerjohn, S. E., Martinson, D. G., Smith, R. C., Yuan, X., and Rind, D.: Trends in Antarctic annual sea ice retreat and advance and their relation to El Nino-Southern Oscillation and Southern Annular Mode variability, J. Geophys. Res., 108, 3329, doi:10.1029/2002JC001543, 2008a.

CPD
9, 1–41, 2013

Stammerjohn, S. E., Martinson, D. G., Smith, R. C., and Iannuzzi, R. A.: Sea ice in the western Antarctic Peninsula region: spatio-temporal variability from ecological and climate change perspectives, Deep-Sea Res. Pt. II, 55, 2041–2058, 2008b.

Steig, E. J.: Climate change: brief but warm Antarctic summer, Nature, 498, 39–41, 2012.

Steig, E. J., Brook, E. J., White, J. W. C., Sucher, C. M., Bender, M. L., Lehman, S. J., Morse, D. L., Waddington, E. D., and Clow, G. D.: Synchronous climate changes in Antarctica and the North Atlantic, Science, 282, 92–95, 1998.

Steig, E. J., Schneider, D. P., Rutherfold, S. D., Mann, M. E., Comiso, J. C., and Shindell, D. T.: Warming of the Antarctic ice-sheet surface since the 1957 International Geophysical year, Nature, 457, 459–463, 2009.

Taylor, F. and Sjunneskog, C.: Postglacial marine diatom record of the Palmer Deep, Antarctic Peninsula (ODP Leg 178, Site 1098) 2; Diatom assemblages, Paleoceanography, 17, 8001, doi:10.1029/2000PA000564, 2002.

Taylor, F., Whitehead, J., and Domack, E.: Holocene paleoclimate change in the Antarctic Peninsula: evidence from the diatom, sedimentary and geochemical record, Mar. Micropaleontol., 41, 25–43, 2001.

Toggweiler, J. R., Russell, J. L., and Carson, S. R.: Mid latitude westerlies, atmospheric CO_2, and climate change during the ice ages, Paleoceanography, 21, PA2005, doi:10.1029/2005PA001154, 2006.

Turner, J.: The El Niño-Southern Oscillation and Antarctica, Int. J. Climatol., 24, 1–31, 2004.

Vaughan, D. G. and Doake, C. S. M.: Recent atmospheric warming and retreat of ice shelves on the Antarctic Peninsula, Nature, 379, 328–331, 1996.

Volkman, J. K., Barrett, S. M., and Dunstan, G. A.: C_{25} and C_{30} highly branchedisoprenoid alkenes in laboratory cultures of two marine diatoms, Org. Geochem., 21, 407–413, 1994.

Weijers, J. W. H., Schouten, S., Spaargaren, O., and Sinninghe Damsté, J. S.: Occurrence and distribution of tetraether membrane lipids in soils: implications for the use of the TEX_{86} proxy and the BIT index, Org. Geochem., 37, 1680–1693, 2006.

Whitehead, J. M., Wotherspoon, S., and Bohaty, S. M.: Minimal Antarctic sea ice during the Pliocene, Geology, 33, 137–140, 2005.

Willmott, V., Rampen, S. W., Domack, E., Canals, M., and Sinninghe Damsté, J. S., and Schouten, S.: Holocene changes in Proboscia diatomproductivity in shelf waters of the northwestern Antarctic Peninsula, Antarct. Sci., 22, 3–10, 2010.

CPD
9, 1–41, 2013

Yoon, H. I., Park, B. K., Kim, Y., and Kan, C. Y.: Glaciomarine sedimentation and its paleoclimatic implications on the Antarctic Peninsula shelf over the last 15 000 years, Palaeogeogr. Palaeocl., 185, 235–254, 2002.

Yuan, X. J.: ENSO-related impacts on Antarctic sea ice: a synthesis of phenomenon and mechanisms, Antarct. Sci, 16, 415–425, 2004.

Yuan, X. J. and Martinson, D. G.: Antarctic sea ice extent variability and its global connectivity, J. Climate, 13, 1697–1717, 2000.

CPD

9, 1–41, 2013

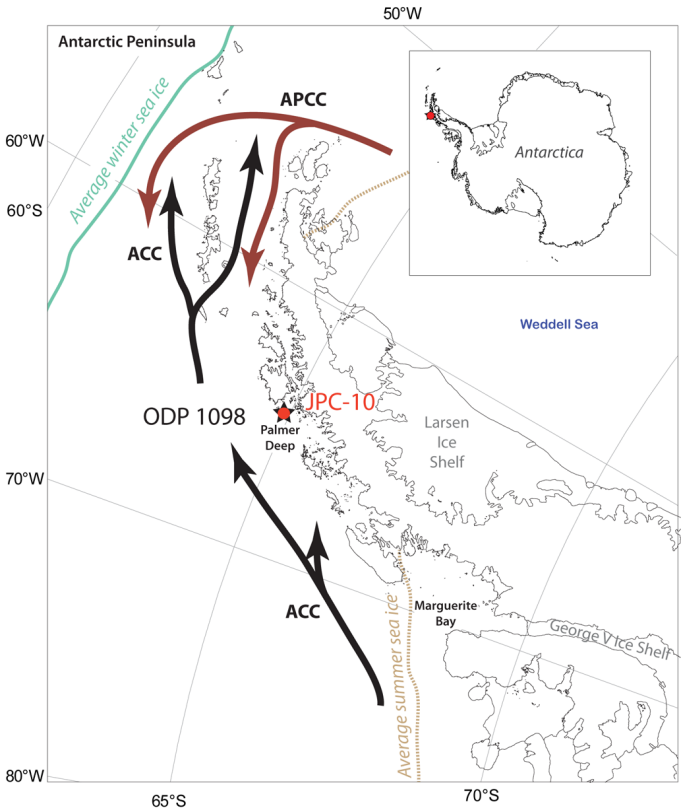

Fig. 1. Location of the JPC-10 core and the ODP Site 1098 in Western Antarctic Peninsula (WAP). The dashed yellow line represents the limit of sea ice presence during the summer while the solid green line delineates the maximum sea ice extent during the winter. Major oceanic currents: ACC, Antarctic Circumpolar Current and APCC, Antarctic Peninsula Circumpolar Countercurrent which is derived from the Weddell Sea surface waters.

CPD
9, 1–41, 2013

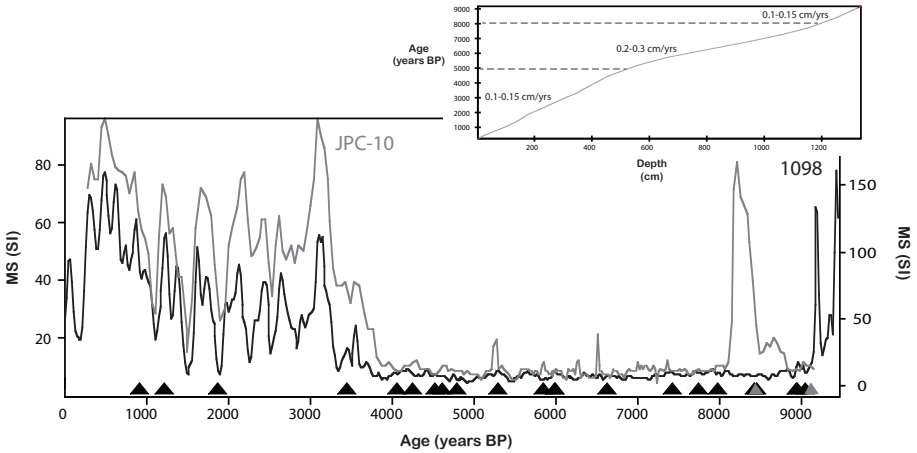

Fig. 2. Age model and sedimentation rate. The main panel represents the MS correlation between the core JPC-10 and the ODP Site 1098. Grey and black markers indicate respective ^{14}C dates for the JPC-10 and Site 1098. The upper, smaller panel shows the sedimentation of core JPC-10.

CPD
9, 1–41, 2013

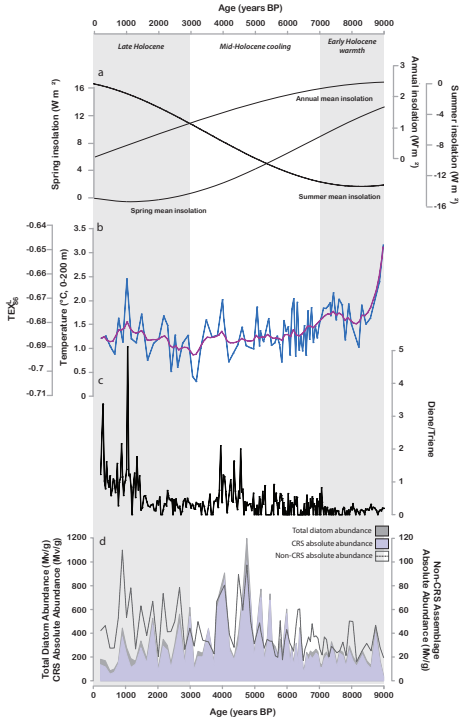

Fig. 3. Paleoclimatic proxies from the core JPC-10 compared with Holocene insolation. **(a)** Annual, summer and spring mean insolation at 65° S (Berger and Loutre, 1991), **(b)** TEX_{86}^{L} index and temperature (°C, 0–200 m) record (blue) and the smoothed curve (red), **(c)** the D/T ratio and **(d)** the total diatom abundance ($Mv\,g^{-1}$), the CRS absolute abundance ($Mv\,g^{-1}$) and the non-CRS assemblage absolute abundance ($Mv\,g^{-1}$). The two vertical solid grey bars denote the early Holocene warmth, mid-Holocene cooling and late Holocene periods.

CPD
9, 1–41, 2013

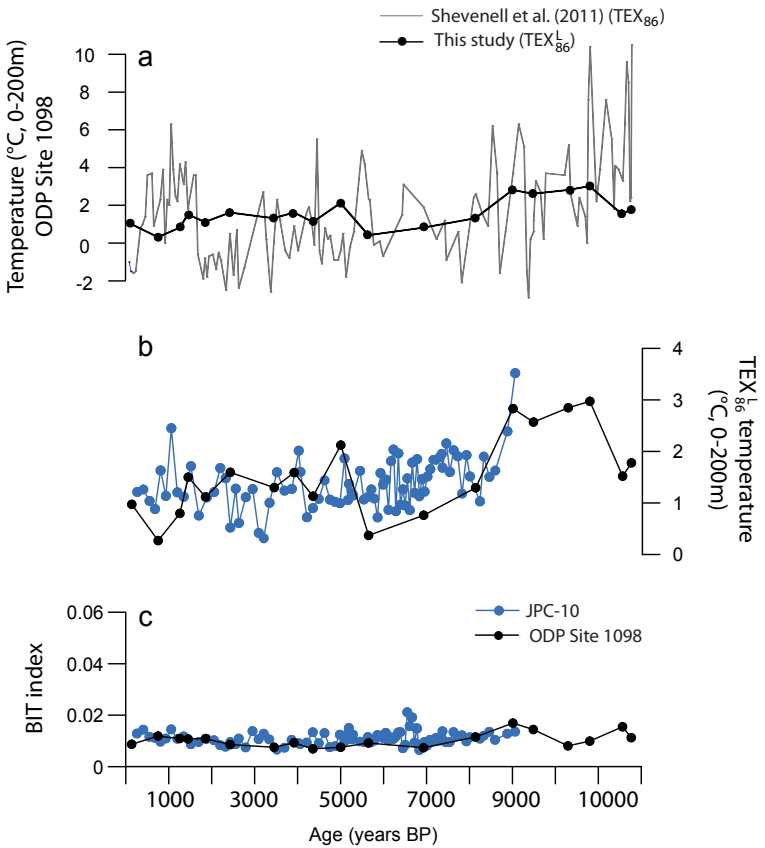

Fig. 4. (a) TEX_{86}^{L} (this study) versus TEX_{86} (shevenell et al. (2011) records at ODP Site 1098. **(b)** JPC-10 and ODP Site 1098 TEX_{86}^{L} records. **(c)** JPC-10 and ODP Site 1098 BIT index records. Note the different temperature scale used between Fig. 4a, b due to the different temperature amplitude resulting of the application of two different indices and two different calibrations.

CPD
9, 1–41, 2013

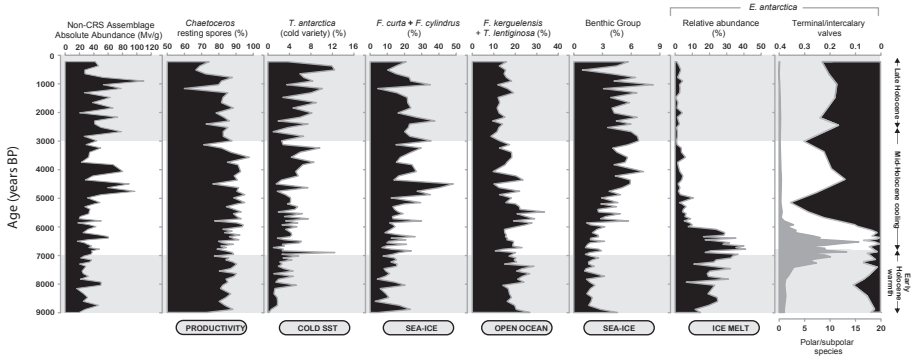

Fig. 5. *Chaetoceros*-free diatom relative abundance (%) of selected environmental indicator species from core JPC-10. On the right panel, the grey curve indicates the ratio between polar and subpolar *E. antarctica* species, while in black is represented the terminal and intercalary valves ratio.

CPD
9, 1–41, 2013

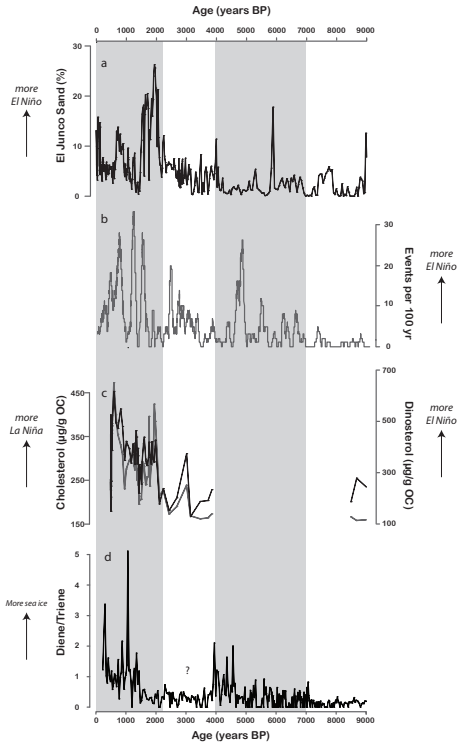

Fig. 6. (a) El Junco Sand (%) (Conroy et al., 2008), **(b)** ENSO frequency (events per 100 yr) (Moy et al., 2002), **(c)** cholesterol and dinosterol concentrations (µg g^{-1} OC) (Makou et al., 2011) and **(d)** D/T ratio records. On this figure is delimited four major phases which represents four different steps in the D/T variations. The most important D/T ratio increase corresponds well to significant ENSO events. Note the absence of ENSO and D/T correlations between ~ 4000 and 2100 yr BP.

CPD
9, 1–41, 2013